SEARCH FOR RESONANT DOUBLE HIGGS PRODUCTION WITH BBZZ DECAYS IN THE $b\bar{b}\ell\ell\nu\bar{\nu}$ FINAL STATE IN pp COLLISIONS AT $\sqrt{s} = 13$ TeV

by

Rami Kamalieddin

A DISSERTATION

Presented to the Faculty of

The Graduate College at the University of Nebraska

In Partial Fulfilment of Requirements

For the Degree of Doctor of Philosophy

Major: Physics and Astronomy

Under the Supervision of Professor Ilya Kravchenko

Lincoln, Nebraska

May, 2019

SEARCH FOR RESONANT DOUBLE HIGGS PRODUCTION WITH BBZZ DECAYS IN THE $b\bar{b}\ell\ell\nu\bar{\nu}$ FINAL STATE IN pp COLLISIONS AT $\sqrt{s} = 13$ TeV

Rami Kamalieddin, Ph.D.

University of Nebraska, 2019

Advisers: Ilya Kravchenko

Since the discovery of the Higgs boson in 2012 by the A Toroidal LHC ApparatuS (ATLAS) and The Compact Muon Solenoid (CMS), most of the quantum mechanical properties that describe the long-awaited Higgs boson have been measured. Due to an impeccable work of the LHC, dozens of fb^{-1} of data have been delivered to both experiments. Finally, it became possible for analyses that have a very low cross section to observe rare decay modes of the Higgs boson, as was done successfully recently in ttH and VHbb channels. The only untouched territory is a double Higgs boson production. Data will not help us much either at the HL-LHC, the process will remain unseen even in the most optimistic scenarios, so one has to rely solely on new reconstruction methods as well as new analysis techniques. This thesis is addressing both goals. I have been blessed by an opportunity to work in the CMS electron identification group, where we have developed new electron identification algorithms. The majority of this thesis, however, will be devoted to the second goal of HL-LHC. We establish the techniques for the first ever analysis at the LHC that searches for the double Higgs production mediated by a heavy narrow-width resonance in the $b\bar{b}ZZ$ channel: $X \to HH \to b\bar{b}ZZ^* \to b\bar{b}\ell\ell\nu\bar{\nu}$. The analysis searches for a resonant production of a Higgs boson pair in the range of masses of the resonant parent particle from 250 to 1000 GeV. Both spin scenarios of the resonance are considered: spin 0 (later called "graviton") and spin 2 (later called "radion"). In the absence of the

evidence of the resonant double Higgs boson production from the previous searches, we set upper confidence limits. When combined with other search channels, this analysis will contribute to the discovery of the double Higgs production and we would be able to finally probe the Higgs boson potential using its self-coupling.

"... a place for a smart quote!"

Lenin, 1922.

ACKNOWLEDGMENTS

This will be a longgggg list!

Table of Contents

List of Figures

List of Tables

0.1 Particle symbols

0.2 Introduction

The Higgs boson discovery in 2012 by the CMS [?] and ATLAS [?] collaborations completed the picture of the standard model (SM) [?, ?, 38] of the particle physics. Most of the basic properties of the Higgs boson have been measured. However, several processes have very low cross sections and it remains difficult to distinguish them from the irreducible SM background processes with a similar signature. One of the important but rare processes is a double Higgs (HH) boson production that is sensitive to the Higgs boson self-coupling, therefore, has an access to the shape of the Higgs boson potential. In the SM HH production is a non-resonant production with a cross section of $\sigma =$ fb [?] at $\sqrt{s} = 13$ TeV. Several Beyond the Standard Model (BSM) theories and models, such as supersymmetry, composite Higgs, Warped Extra Dimensions (WED) [?, 6–8, 10], predict scenarios of the enhanced double Higgs boson cross section. There may be two cases: a non-resonant production, introducing BSM terms to the SM lagrangian or a resonant production, in which the process is mediated by a narrow width resonance [?].

In this analysis we examine the resonant di-Higgs production through the gluon fusion mechanism mediated by a heavy narrow resonance, such as RS1 KK graviton or RS1 radion ("graviton" or "radion" later in the text) [?, ?, ?]. The analysis is performed for masses of graviton/radion from 250 GeV to 1000 GeV. 95 % upper confidence limits are set on the production of the graviton with a subsequent decay to Higgs bosons times the branching ratios of the Higgs bosons decaying to a pair of b quarks and the other Higgs boson to two leptons and two neutrinos respectively (Fig. 0.1). With the given data and evaluated uncertainties, the results are compatible with the Standard Model.

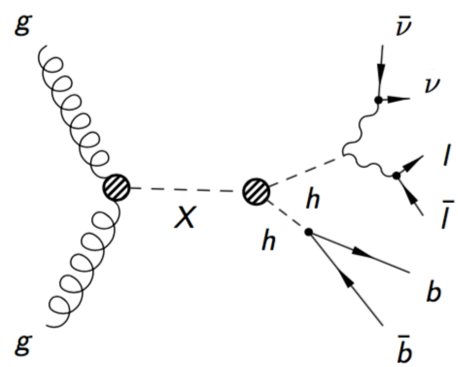

Figure 0.1: The Feynman diagram of the graviton production with the subsequent decay to a pair of the Higgs bosons. What follows is a decay to a pair of b quarks and Z bosons. Shown is 2 b quarks, 2 leptons, and 2 neutrinos final state.

0.2.1 Analysis Strategy

The analysis is based on ntuples and object selection from the approved VHbb sister analysis [**?**]. Leptons, b jets, and the missing transverse energy (MET) are reconstructed using the standard CMS procedures [**?**] and the Particle Flow (PF) algorithm [**?**]. b-jets are identified using the Combined MVA v2 (CMVA) algorithm [**?**]. Then, on shell Z bosons are selected of dilepton pairs with a net charge zero for a pair. Higgs boson decaying to b quarks (Hbb) is reconstructed as a pair of b jets with the highest CMVA output value. Finally, double Higgs boson transverse mass, which is used in the shape analysis to extract limits, is constructed computing the transverse mass of the sum of the Lorentz vectors of the two leptons forming the on-shell Z, MET, and a pair of the b jets forming the H $\rightarrow b\bar{b}$. An additional cut on the missing transverse energy preserves the orthogonality with the existing HIG-18-013 “2b 2l 2q” analysis. Lastly, the cut on the BDT is used to reduce the background contamination in the signal region.

Main backgrounds are $t\bar{t}$ and Drell-Yan in association with jets. Their normalization is extracted during the simultaneous fit of signal region (SR), as well as control region $t\bar{t}$ (CRTT), and control region Drell-Yan (CRDY). Others, minor backgrounds, are single top production, diboson samples (WW, WZ, ZZ), and ZH production.

0.3 Data and Triggers

0.3.1 Data

This measurement uses the full dataset of 2016 collected with the CMS detector in pp collisions at 13 TeV center-of-mass energy with the corresponding integrated lumonocity of 35.9 fb^{-1}.

As the measurement is based on dilepton signatures, the DoubleMuon and DoubleElectron primary datasets are analyzed and only on-shell $Z(\ell\ell)$decays are considered, where $\ell =,$.

The run periods and the corresponding integrated luminosities are listed in Table 0.1 for DoubleMuon channel, DoubleElectron channel is similar.

Table 0.1: List of used 2016 DoubleMuon data sets. An uncertainty of 2.5% is assigned for the 2016 data set luminosity [**?**]

Dataset	$\int L$ (fb^{-1})
DoubleMuon__Run2016B-03Feb2017-v2	∼5.9
DoubleMuon__Run2016C-03Feb2017-v1	∼2.7
DoubleMuon__Run2016D-03Feb2017-v1	∼4.3
DoubleMuon__Run2016E-03Feb2017-v1	∼4.1
DoubleMuon__Run2016F-03Feb2017-v1	∼3.2
DoubleMuon__Run2016G-03Feb2017-v1	∼3.8
DoubleMuon__Run2016H-03Feb2017-v1	∼11.8
Total Lumi	35.9

0.3.2 Triggers

Because the analysis is performed in the dielectron and dimuon channels, unprescaled dilepton triggers with the lowest available transverse momentum thresholds are utilized. The triggers at the L1 and HLT level are listed in Table 0.2. Dielectron trigger requires the leading electron to pass 23 GeV p_T cut and 12 GeV p_T cut for the subleading electron, both electrons should be within $\eta < 2.5$. Dimuon triggers require the leading muon to pass 17 GeV p_T cut and 8 GeV p_T cut for the subleading muon, both muons should be within $\eta < 2.4$. η region in the gap is excluded (1.4442 to 1.566).

Before measuring trigger scale factors, ID and ISO cuts are applied, as well as p_T cuts of the offline selection. For dielectron trigger leading and subleading electrons have to pass 25 GeV p_T cut and 15 GeV p_T cut correspondinly. Dimuon triggers require the leading muon to pass 20 GeV p_T cut and 15 GeV p_T cut for the subleading muon. Dilepton scale factor have been computed for each leg separately, since the cuts on each leg vary (Fig. 0.2). Following the recommendations from the Muon POG, scale factors have been computed separately for two groups: run H and other runs, and then the luminosity averaged scale factors are calculated (Figs. 0.3, 0.4, 0.5).

Table 0.2: Triggers for dimuon and dielectron analysis channels both at L1 and HLT levels.

Channel	L1 Seeds	HLT Paths
Z() Z()H $\rightarrow b\bar{b}$	L1_SingleMu20	HLT_Mu17_TrkIsoVVL_Mu8_TrkIsoVVL_v* OR HLT_Mu17_TrkIsoVVL_TkMu8_TrkIsoVVL_v* OR HLT_Mu17_TrkIsoVVL_Mu8_TrkIsoVVL_DZ_v* OR HLT_Mu17_TrkIsoVVL_TkMu8_TrkIsoVVL_DZ_v*
Z() Z()H $\rightarrow b\bar{b}$	L1_SingleEG30 OR L1_SingleIsoEG22er OR L1_SingleIsoEG24 OR L1_DoubleEG_15_10	HLT_Ele23_Ele12_CaloIdL_TrackIdL_IsoVL_DZ

[][Leg 1]

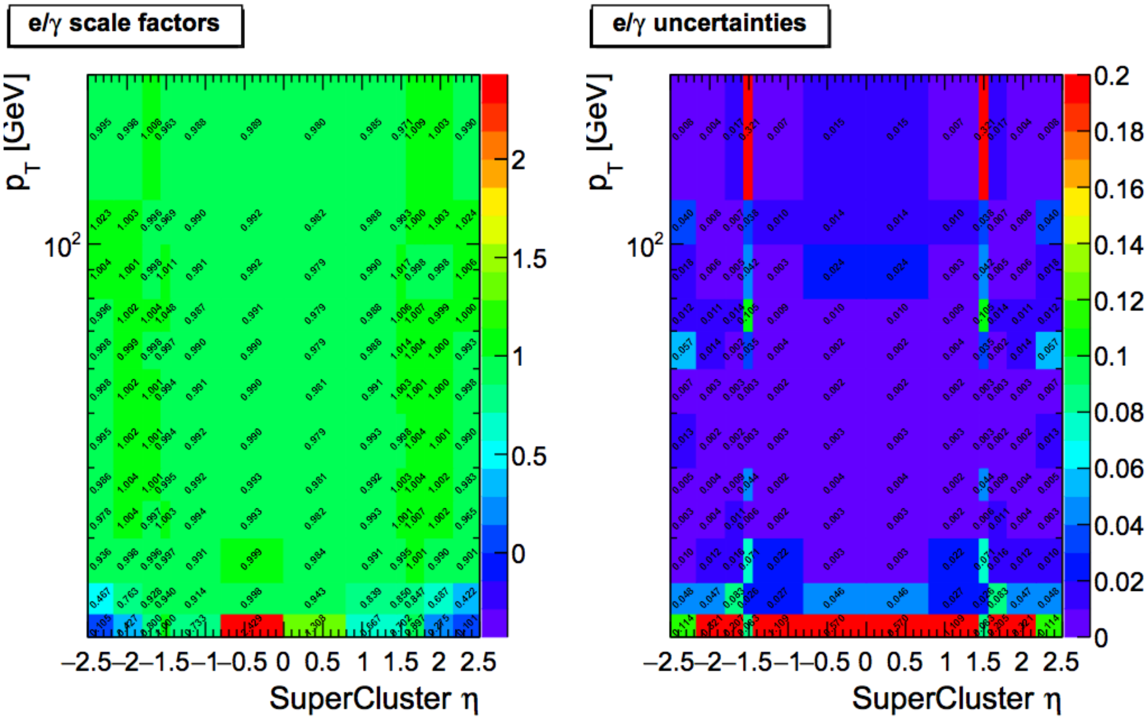

[][Leg 2]

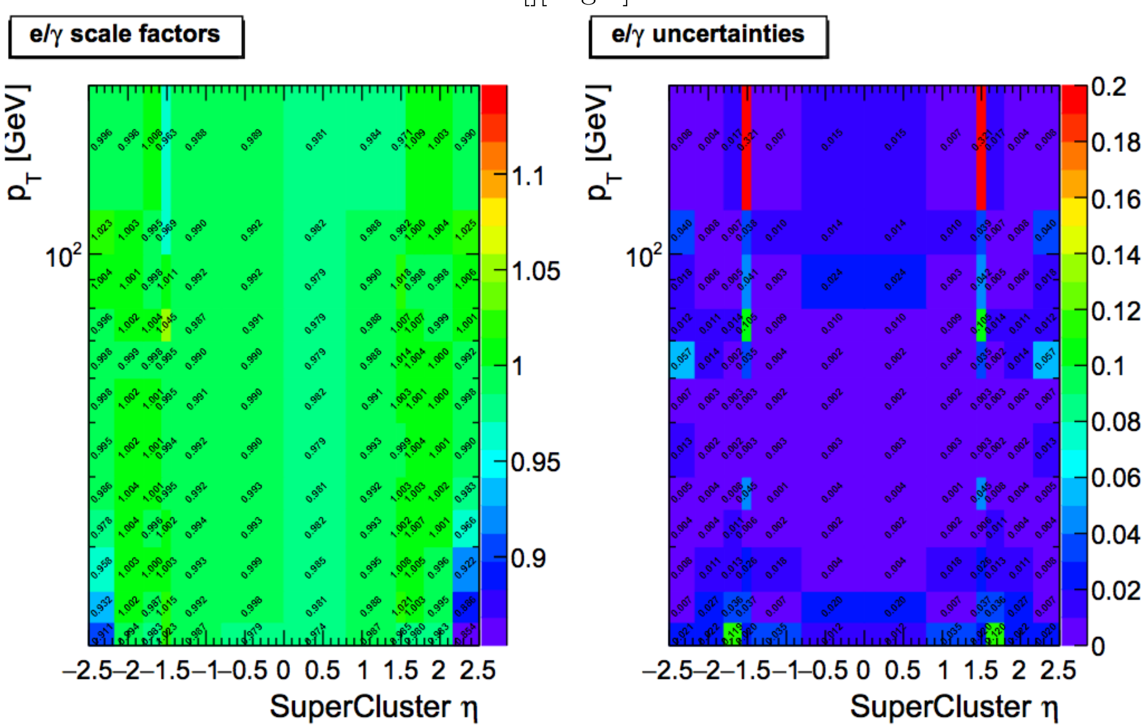

Figure 0.2: Electron scale factors in p_T and η bins for 2016 data set for the HLT_Ele23_Ele12_CaloIdL_TrackIdL_IsoVL_DZ trigger. ID cut (general purpose MVA WP90) and ISO cuts are applied, then the scale factors are measured. Taken from [**?**]

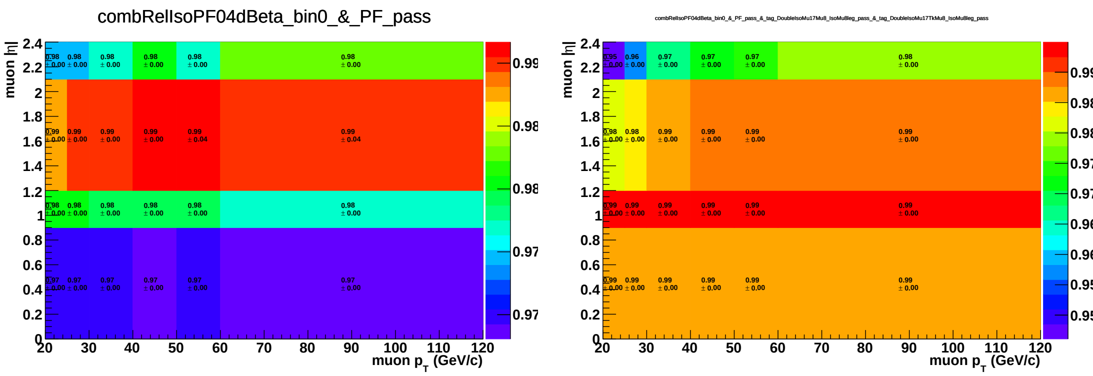

Figure 0.3: Muon scale factors in p_T and η bins for 2016 data runs B, C, D, E, F, G for the HLT_Mu17_TrkIsoVVL_Mu8_TrkIsoVVL_v* OR HLT_Mu17_TrkIsoVVL_TkMu8_TrkIs oVVL_v* triggers. Left: Scale factors for 8 GeV leg. Right: Scale factors for 17 GeV leg, provided that the subleading leg passed 8 GeV cut.

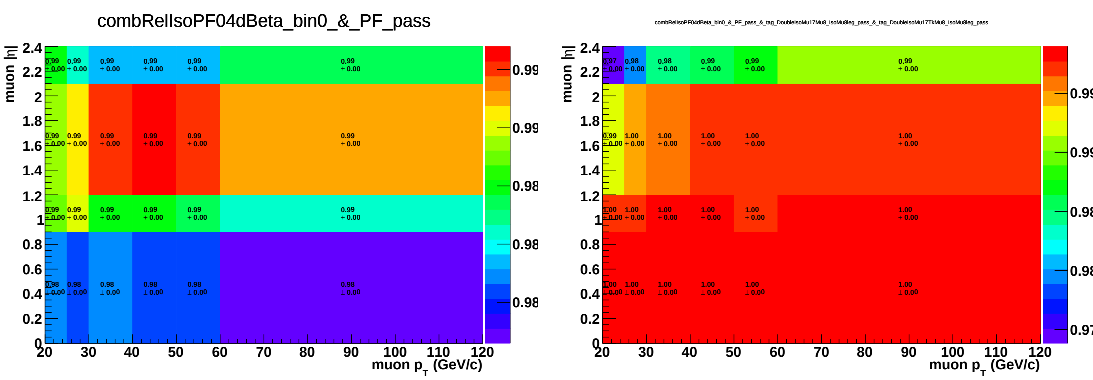

Figure 0.4: Muon scale factors in p_T and η bins for 2016 data run H for the HLT_Mu17_TrkIsoVVL_Mu8_TrkIsoVVL_v* OR HLT_Mu17_TrkIsoVVL_TkMu8_TrkIs oVVL_v* triggers. Left: Scale factors for 8 GeV leg. Right: Scale factors for 17 GeV leg, provided that the subleading leg passed 8 GeV cut.

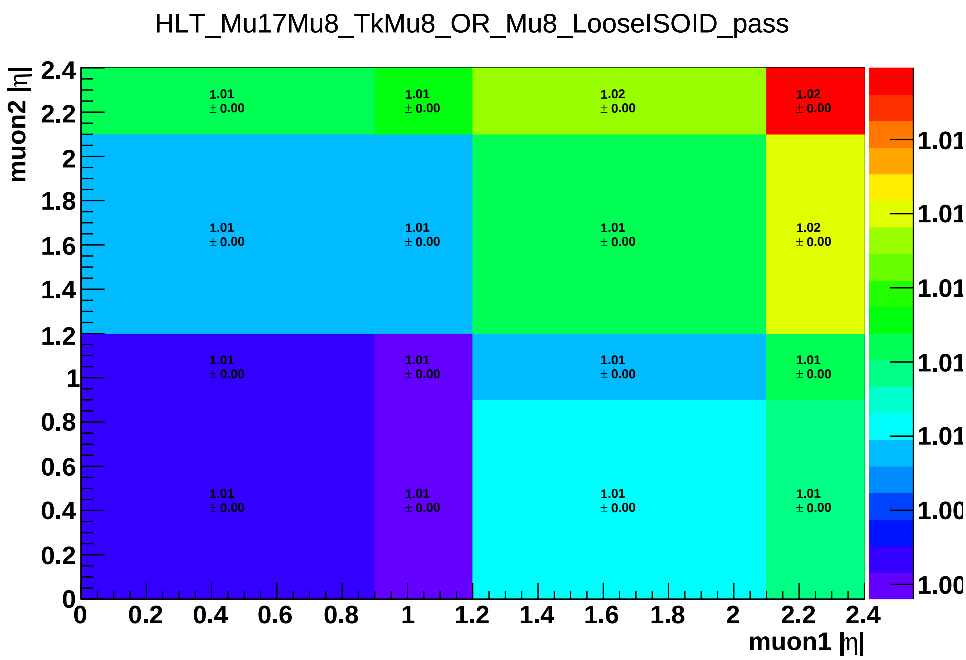

Figure 0.5: Scale factors in η bins of the leading and subleading muons for 2016 data set for dZ requirement, measured after muons have passed the HLT_Mu17_TrkIsoVVL_Mu8_TrkIsoVVL_v* OR HLT_Mu17_TrkIsoVVL_TkMu8_TrkIsoVVL_v* triggers.

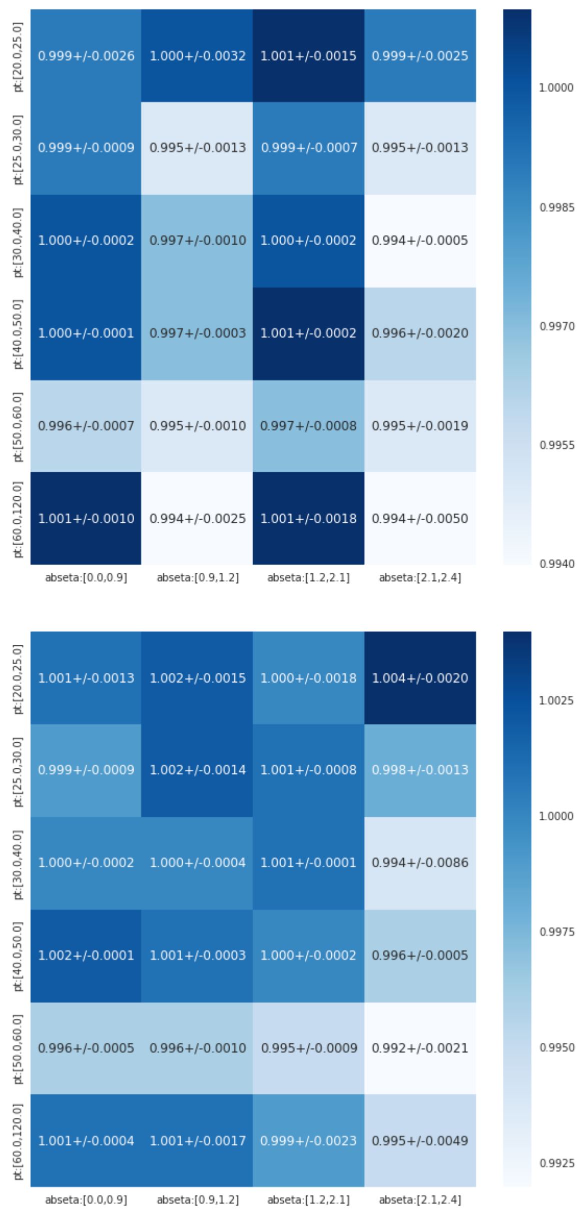

Figure 0.6: Muon ID scale factors in p_T and η bins. Left: runs B to F. Right: runs G and H.

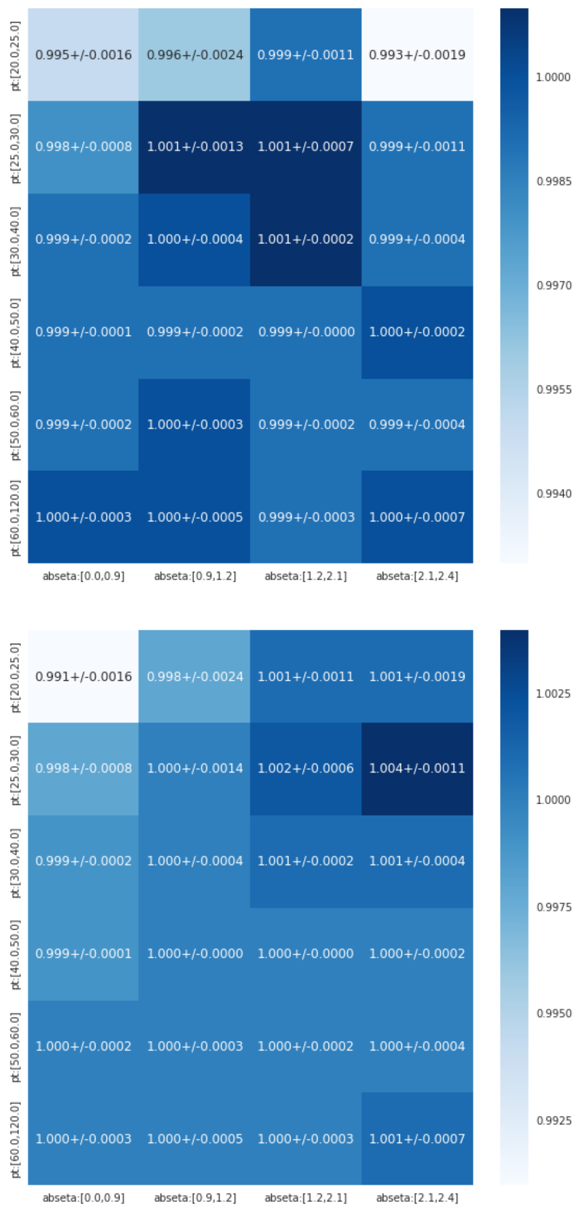

Figure 0.7: Muon ISO scale factors in p_T and η bins. Left: runs B to F. Right: runs G and H.

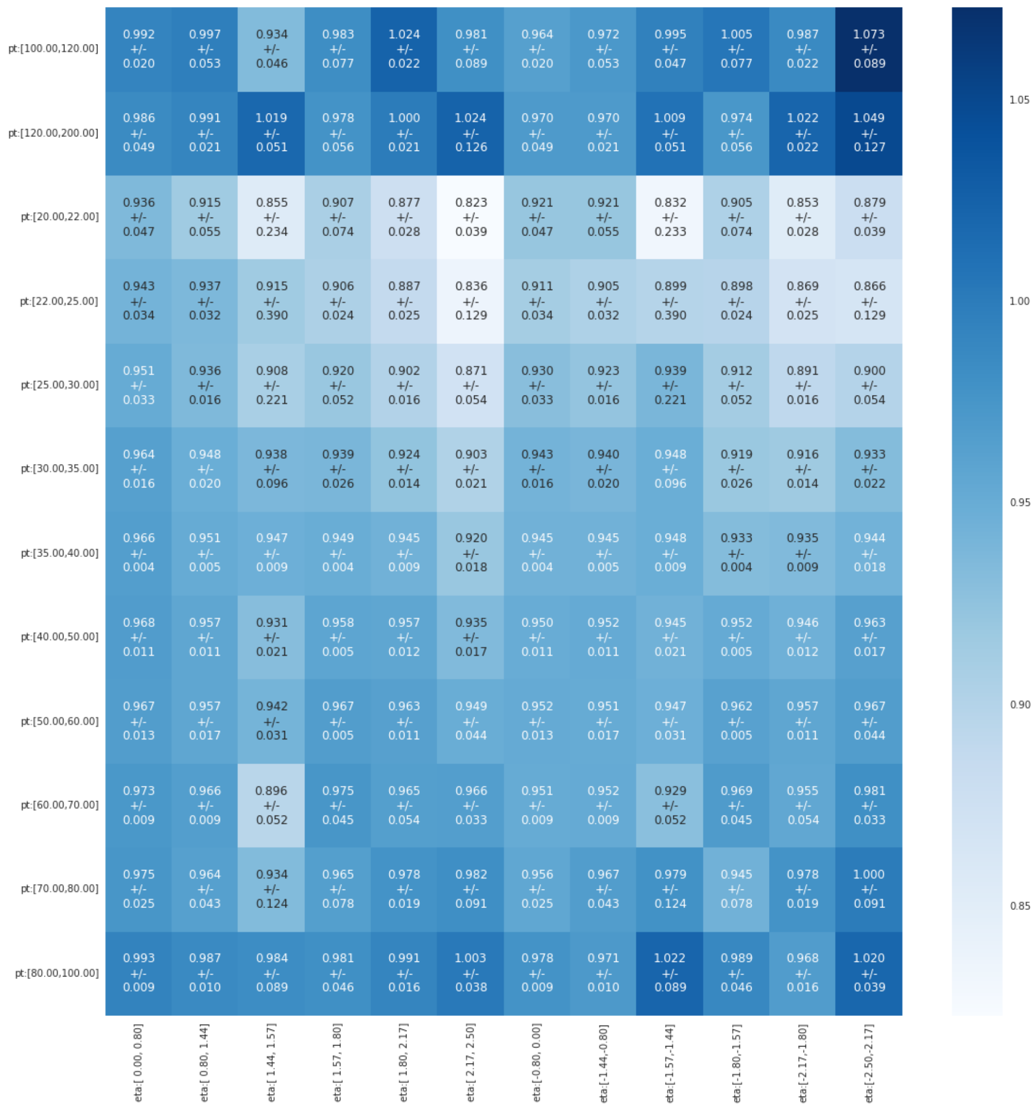

Figure 0.8: Electron ID+ISO scale factors in p_T and η bins.

0.4 Simulated Samples

0.4.1 Signal simulation

The resonant Monte Carlo (MC) signal samples of the Higgs boson pair production have been generated at the Leading Order (LO) using the 5 version 2.2.2.0 generator [**?**]. The gluon fusion production of a heavy narrow resonance is followed by the decay of the resonance into two Higgs bosons whose mass is set to 125 GeV.

Two signal MC samples are generated to cover the Higgs decay modes contributing to the final state of this measurement. In the first sample ("bbZZ"), one Higgs boson decays to a pair of b-quarks and the second decays into two Z bosons. In the second sample ("bbVV"), one of the Higgs bosons decays to two b-quarks while the other decays into a pair of W or a pair of Z bosons. For both samples, both the Z boson-pair and the W boson-pair are set to decay leptonically to two leptons and two neutrinos, where a lepton could be an electron or a muon. The second, bbVV, sample is filtered according to the generator level information and only the events with a W-boson pair ("bbWW") are kept, while the Z-pair events are dropped as there are very few of them in the bbVV sample.

Events in the bbZZ and bbWW MC samples are assigned weights to obtain predicted signal yields for the integrated luminosity of the data set of this measurement using the value for the HH production cross section of 2 pb, a value of the order of predicted enhanced cross sections in typical BSM theories with such resonances. The weights incorporate the branching ratios of the Higgs boson decays contributing to the final state studied here: 0.0012 and 0.0266 for $HH \to bbZZ \to bb\ell\ell\nu\nu$ and $HH \to bbWW \to bb\ell\nu\ell\nu$, respectively [**?**].

Unless mentioned otherwise, throughout the text plots and numbers represent the graviton study. The data and backgrounds for the radion measurement are the same, thus distributions also show the same good Data MC behavior and can be found for at Figs. ?? for the graviton case and ?? for the rad ion case.

0.4.2 Background simulation

In this analysis the main backgrounds are $t\bar{t}$ and Drell-Yan plus jets with the mass of the boson greater than 50 GeV. Not all the background pass our preselection (see section those which do, are single top, dibosons, and ZH backgrounds that are listed in the Table 0.3:

Table 0.3: Background Monte Carlo samples

DY1JetsToLL_M-50_TuneCUETP8M1_13TeV-madgraphMLM-pythia8
DY2JetsToLL_M-50_TuneCUETP8M1_13TeV-madgraphMLM-pythia8
DY3JetsToLL_M-50_TuneCUETP8M1_13TeV-madgraphMLM-pythia8
DY4JetsToLL_M-50_TuneCUETP8M1_13TeV-madgraphMLM-pythia8
WW_TuneCUETP8M1_13TeV-pythia8
WZ_TuneCUETP8M1_13TeV-pythia8
ZZ_TuneCUETP8M1_13TeV-pythia8
ZH_HToBB_ZToLL_M125_13TeV_aMC@NLO
TT_TuneCUETP8M1_13TeV-powheg-pythia8
ST_tW_top_5f_inclusiveDecays_13TeV-powheg-pythia8_TuneCUETP8M1
ST_tW_antitop_5f_inclusiveDecays_13TeV-powheg-pythia8_TuneCUETP8M1
ST_t-channel_top_4f_leptonDecays_13TeV-powheg-pythia8
ST_t-channel_antitop_4f_leptonDecays_13TeV-powheg-pythia8
ST_s-channel_4f_leptonDecays_13TeV-amcatnlo-pythia8

The simulated samples of the background processes, $t\bar{t}$ [?] and the single top tW and t-channel production processes [?], are generated at the next-to-leading order (NLO) with POWHEG [?], while single top s-channel production process is generated at NLO with . $t\bar{t}$ and single top production cross sections are rescaled to the next-to-next-to-leading order (NNLO). Drell-Yan (DY) process samples in association with 1, 2, 3 or 4 jets, are generated at the leading order using with the MLM matching [?] and rescaled to NNLO using FEWZ program [?, ?, ?]. As for the EWK order, DY samples have been rescaled to EWK NLO order with the NLO/LO k-factor of 1.23 [?]. Diboson samples are generated at LO with 8.212 [?].

The main background process, which involves SM Higgs boson, is an associated production of the Higgs boson with a Z boson (ZH). ZH process is simultated using the generator $MadGraph5\_aMC@NLO$ [?] with FxFx merging [?] and rescaled to NNLO with generator [?].

For LO and NLO samples NNPDF3.0 parton distribution functions (PDF) set is used. and interfaced with 8.212 [?] are used for the parton showering and hadronization steps. To describe the underlying event CUETP9M1 set derived in [?] is used. [?] is used to model the response of the CMS detector.

All the final cross sections denoted as NNLO are calculated at NNLO QCD accuracies and have been computed with the tool they were generated with. They found to be in agreement with the values from the LHC Higgs cross section working group [?, ?, ?, ?, ?].

During the data taking in 2016 the average number of proton-proton intercations per bunch crossing was 24 (denoted as pile up later), and MC samples contain this information overlaping these interactions with the events of interest.

0.5 Physics Objects Reconstruction

0.6 Event Selection

0.7 BDT Discriminant

0.8 Systematic Uncertainties

0.9 Statistical Analysis

0.10 Limits Extraction

0.11 Conclusions